A novel anthraquinone-quinazoline hybrid 7B blocks breast cancer metastasis and EMT via targeting EGFR and Rac1

JIANKANG KANG[1*], YANPING ZHONG[1*], WEI TIAN[2], JUNYING LI[2], XINXIAO LI[1], LINA ZHAI[1], HUAXIN HOU[2] and DANRONG LI[1]

[1]Life Sciences Institute and [2]College of Pharmacy, Guangxi Medical University, Nanning, Guangxi Zhuang Autonomous Region 530021, P.R. China

Received August 30, 2020; Accepted February 9, 2021

DOI: 10.3892/ijo.2021.5199

Abstract. At present, effective therapeutic drugs for triple-negative breast cancer (TNBC) are lacking due to the absence of identified or available targets. Therefore, the present study aimed to identify key molecular targets and a specific targeted therapeutic drug to aid with the development of novel therapeutic strategies for TNBC. Based on the high expression of EGFR and Rac1 in TNBC and inspired by a novel antitumor strategy termed combi-targeting, novel anthraquinone-quinazoline hybrid 7B was synthesized to simultaneously target EGFR and Rac1. It was hypothesized that hybrid 7B may possess enhanced potency compared with its parent compounds. Breast cancer cell viability was detected by performing MTT assays. Flow cytometry was conducted to detect the effects of hybrid 7B on the cell cycle, apoptosis and the mitochondrial outer membrane potential. Ultrastructural alterations were observed by transmission electron microscopy. Cell invasion and migration were assessed by performing Transwell and wound-healing assays, respectively. The expression levels of epithelial-mesenchymal transition (EMT) markers and metastasis-related proteins were detected by western blotting. Compared with Rhein and gefitinib, hybrid 7B displayed superior antiproliferative activity in MDA-MB-231 cells with an IC_{50} value of 2.31 μM, which was 14-fold higher compared with the EGFR tyrosine kinase inhibitor gefitinib. Further experiments demonstrated that hybrid 7B significantly reduced the mitochondrial membrane potential, enhanced MDA-MB-231 cell apoptosis and induced cell cycle arrest at the G_2/M phase compared with the control group. Typical morphological alterations of apoptotic cells were observed in hybrid 7B-treated MDA-MB-231 and MCF-7 cells. Compared with the control group, hybrid 7B significantly inhibited MDA-MB-231 cell invasion and migration by downregulating Rac1, EGFR, matrix metalloproteinases, snail family transcriptional repressor 1, Vimentin and β-catenin protein expression levels, and upregulating E-cadherin protein expression levels. The present study demonstrated that hybrid 7B inhibited TNBC cell migration and invasion by reversing EMT and targeting EGFR and Rac1; therefore, hybrid 7B may serve as a promising therapeutic agent for TNBC.

Introduction

Triple-negative breast cancer (TNBC) is one of the most aggressive subtypes of breast cancer, due to its high invasiveness, high recurrence and poor prognosis (1). At present, there is a lack of effective therapeutic targets and drugs for the clinical treatment of TNBC. Different proteins are expressed in various types of breast cancer cells, including epidermal growth factor receptor (EGFR), which is overexpressed in MDA-MB-231 cells, but lowly expressed in MCF-7 cells (2). Therefore, identifying key molecular targets and developing specific targeted therapeutic drugs is important for the development of novel therapeutic strategies for TNBC.

EGFR, a member of the EGFR family, is involved in tumor cell proliferation, angiogenesis, tumor invasion and metastasis (3). EGFR is abnormally expressed in several solid tumors, including TNBC (4). Among all TNBC cases, 50-75% are associated with EGFR activation or overexpression (5). Due to the multidimensional role of EGFR in the progression of cancer, targeting EGFR has emerged as a potential anticancer therapeutic strategy.

Correspondence to: Professor Huaxin Hou, College of Pharmacy, Guangxi Medical University, 22 Shuangyong Road, Nanning, Guangxi Zhuang Autonomous Region 530021, P.R. China
E-mail: houhuaxin@163.com

Professor Danrong Li, Life Sciences Institute, Guangxi Medical University, 22 Shuangyong Road, Nanning, Guangxi Zhuang Autonomous Region 530021, P.R. China
E-mail: danrongli@163.com

*Contributed equally

Abbreviations: EMT, epithelial-mesenchymal transition; MMP, mitochondrial membrane potential; MOE, Molecular Operating Environment; TEM, transmission electron microscopy; TNBC, triple negative breast cancer; TKI, tyrosine kinase inhibitor

Key words: anthraquinone-quinazoline hybrid, metastasis, EMT, TNBC, EGFR, Rac1

Rac1 is involved in the regulation of various cellular processes, including adhesion, migration, proliferation, transcription, vesicle formation and cell apoptosis (6). Increasing evidence has demonstrated that Rac1 is abnormally expressed and aberrant Rho family signaling contributes to angiogenesis, invasion and metastasis. Patients with high Rac1 expression levels were more susceptible to early tumor recurrence and displayed poor prognosis (7). Our previous study demonstrated that RP-4, a novel anthraquinone derivative, enhanced the sensitivity of nasopharyngeal carcinoma cells to radiotherapy by targeting Rac1 (8). Rhein can inhibit the production of matrix metallopeptpidase (MMP) by regulating the Rac1/reactive oxygen species/MAPK/activator protein 1 signaling pathway in human ovarian carcinoma cells (9). Several quinazoline derivatives were used as first- and second-generation EGFR tyrosine kinase inhibitors, including gefitinib and afatinib (10). Inspired by anthraquinone and quinazoline derivatives, a series of novel anthraquinone-quinazoline hybrids, which were expected to be more potent antitumor agents by inhibiting the activity of EGFR and Rac1, were designed and synthesized in our previous study (11). Among these hybrids, hybrid 7B displayed antiproliferative activity on several tumor cells, especially on human MDA-MB-231 TNBC cells. However, the effect of hybrid 7B on tumor metastasis and invasion is not completely understood. The present study investigated whether hybrid 7B suppressed breast cancer cell invasion and epithelial-mesenchymal transition (EMT) by downregulating the expression of EGFR and Rac1. The results indicated that targeting both EGFR and Rac1 might serve as a novel and effective therapeutic strategy for TNBC.

Materials and methods

Drugs and reagents. 4,5-Bis(benzyloxy)-9,10-dioxo-N-(4-(3-methy-lphenylamino)quinazolin-6-yl)anthracene-2-carboxamide [hybrid 7B; purity, >98%] had previously been synthesized by our team (11). Hybrid 7B was dissolved in DMSO to make a 5,000 μM stock solution, which was diluted according to the experimental requirements. Rhein was purchased from Nanjing Langze Pharmaceutical Technology Co., Ltd. Gefitinib is purchased from Qilu Pharmaceutical Co., Ltd. DMEM and FBS were purchased from Gibco (Thermo Fisher Scientific, Inc.). EGF was purchased from R&D Systems China Co., Ltd. MTT was purchased from Merck KGaA. Crystal violet dye solution was obtained from Beyotime Institute of Biotechnology. Transwell chambers, Matrigel and the Annexin V-allophycocyanin (APC)/7-aminoactinomycin D (7-AAD) kit were purchased from BD Biosciences.

Cell culture. MDA-MB-231, MCF-7 and MCF-10A cells were purchased from China Center for Type Culture Collection. Cells were cultured in DMEM supplemented with 10% FBS at 37˚C with 5% CO_2.

Cell viability. Cell viability was determined by performing MTT assays. Cells were inoculated ($5x10^3$ cells/well) into a 96-well plate for 24 h. Cells were incubated with or without different concentrations of hybrid 7B [0 (control), 0.5, 1, 2, 4, 8 or 16 μM], rhein [0 (control), 16, 32, 64, 128 or 256 μM] and gefitinib [0 (control), 4, 8, 16, 32 or 64 μM) at 37˚C for 48 h. Subsequently, cells were incubated with 20 μl MTT (5 mg/ml) for 4 h. The cell medium was discarded and 100 μl DMSO was added to each well for 15 min with gentle agitation. Absorbance was measured at a wavelength of 490 nm using a microplate reader (BioTek Instruments, Inc.). Relative cell viability was calculated according to the following formula: Cell viability (%) = (mean absorbance of the test wells/mean absorbance of the control wells) x100. The IC_{30}, IC_{50} and IC_{70} values were calculated as the concentrations of hybrid 7B that inhibited cell viability by 30, 50 and 70%, respectively.

Apoptosis detection. Cell apoptosis was detected using an Annexin V-APC/7-AAD kit. Cells were seeded ($3x10^5$ cells/well) into a 6-well plate. MDA-MB-231 cells were treated with different concentrations of hybrid 7B (0, 1, 2 or 4 μM) for 48 h. MCF-7 cells were treated with hybrid 7B (0, 4, 8 or 16 μM) for 48 h. Following washing twice with PBS, cells were digested with trypsin and centrifuged at room temperature for 5 min at 132 x g. Cells were collected and the supernatant was discarded. Cells were resuspended in 100 μl binding buffer. Subsequently, cells were incubated with 5 μl 7-AAD and 5 μl Annexin V-APC in the dark at room temperature for 30 min. Apoptotic cells (early and late apoptosis) were analyzed using a FACSCalibur flow cytometer (Becton, Dickinson and Company) and Cell Quest Pro software (version 6.0; Becton, Dickinson and Company).

Cell cycle. Cells were seeded ($3x10^5$ cells/well) into a 6-well plate. MDA-MB-231 cells were treated with different concentrations of hybrid 7B (0, 1, 2 or 4 μM) for 48 h. MCF-7 cells were treated with different concentrations of hybrid 7B (0, 4, 8 or 16 μM) for 48 h. Following washing with PBS, cells were digested with trypsin and centrifuged at room temperature for 5 min at 132 x g. Cells were washed twice with precooled PBS and fixed with 70% precooled ethanol at 4˚C overnight. Subsequently, cells were centrifuged (132 x g for 5 min at 25˚C), the supernatant was discarded and 5 ml PBS was added to cells, gently mixed and incubated for 15 min. Following centrifugation (132 x g for 5 min at 25˚C) and discarding the supernatant, 1 ml DNA staining solution was added [Hangzhou Multisciences (Lianke) Biotech Co., Ltd.]. Cells were oscillated for 10 sec and incubated for 30 min at room temperature in the dark. Cell cycle distribution was analyzed using a FACSCalibur flow cytometer (Becton, Dickinson and Company) and ModFit LT software (version 3.0; Verity Software House, Inc.).

Transmission electron microscopy (TEM). MDA-MB-231 and MCF-F cells ($2.5x10^5$ cells/well; 6-well plate) were treated with 2 or 8 μM hybrid 7B for 48 h, respectively. Cells were harvested by centrifugation (132 x g at 5 min at 25˚C) and fixed with 3% glutaraldehyde (1 ml) at 4˚C for 2 h. Subsequently, 1% osmium tetroxide buffer solution was added to fix the sample at 4˚C for 1 h. Cells were dehydrated using an ethanol gradient (30, 50, 70, 90 and 100%; 10 min per step; 25˚C). Subsequently, cells were washed three times with 100% acetone (10 min per wash; 25˚C). Acetone and resin were permeated for 2 h at 25˚C at ratios of 3:1, 1:1 and 1:3. The

last ratio was permeated overnight, and then infiltrated with complete resin for 24 h at 25˚C. Samples were embedded in resin and placed into the oven (40˚C for 15 h, 48˚C for 13 h, 60˚C for 24 h). Ultrathin sections were stained with uranyl acetate for 2 h at 25˚C, followed by lead citrate for 15 min at 25˚C. Cell ultrastructure was observed and photographed by TEM using a H7650 transmission electron microscope (Hitachi, Ltd.).

Mitochondrial membrane potential detection. MDA-MB-231 cells ($2.5x10^5$ cells/well; 6-well plate) treated with hybrid 7B (0, 1, 2 or 4 μM) for 48 h. MCF-7 cells ($2.5x10^5$ cells/well; 6-well plate) were treated with hybrid 7B (4, 8 or 16 μM) for 48 h. Subsequently, cells were digested, collected, centrifuged (132 x g for 5 min at 25˚C) and resuspended in 0.5 ml medium. Cells were incubated with 0.5 ml JC-1 working solution at 37˚C for 20 min. Subsequently, centrifugation was performed at 600 x g for 3-4 min at 4˚C to precipitate cells. The supernatant was discarded and cells were washed twice with ice-cold JC-1 staining buffer. Following centrifugation (132 x g for 5 min at 25˚C), cells were resuspended with JC-1 staining buffer, passed through a 400-mesh nylon screen and detected via flow cytometry using a FACSCalibur flow cytometer (Becton, Dickinson and Company) and CellQuest Pro software (version 6.0; Becton, Dickinson and Company).

Cell invasion assay. Cell invasion was evaluated using a 24-well Transwell chamber (diameter, 6.5 mm; pore size, 8 μm; Corning, Inc.). Each chamber was coated with Matrigel (diluted 1:8 in serum-free medium) at 37˚C for 3 h. To compare the invasive ability between MCF-7 and MDA-MB-231 cells, MDA-MB-231 or MCF-7 cells were inoculated ($4x10^4$ cells/well) into the upper chamber. To assess the effect of hybrid 7B on cell invasion, MDA-MB-231 cells were inoculated in serum-free medium with different concentrations of hybrid 7B (0, 0.25, 0.5 or 1 μM) in the upper chamber. In the lower chamber, 500 μl medium supplemented with 20% FBS was plated in the lower chamber. Following incubation for 48 h at 37˚C, the upper chamber was removed and cells on the surface of the membrane were gently wiped off using cotton swabs, The membrane was fixed with 4% paraformaldehyde at 25˚C for 15 min, then stained with 0.2% crystal purple at 25˚C for 2 min. Invading cells were visualized using a light microscope and analyzed using ImageJ software (version 1.8.0; National Institutes of Health).

Wound-healing assay. MDA-MB-231 cells were incubated in a 6-well plate. Once a fusion monolayer had formed, a plastic pipette tip was used to wound the monolayer. Cell medium was discarded and replaced with medium containing 2% FBS and different concentrations of hybrid 7B (0.25, 0.5 or 1 μM) for 48 h. The wounds were observed using an light microscope in five randomly selected fields of view. The following formula was used to calculate wound closure: Wound closure (%) = [(the width of wound at 0 h-the width of wound at 48 h)/the width of wound at 0 h] x100.

Western blotting. Following treatment with different concentrations of hybrid 7B (MDA-MB-231 cells, 1 or 2 μM; MCF-7 cells, 4 or 8 μM) or gefitinib (MDA-MB-231, 2 μM; MCF-7, 8 μM) for 48 h at 37˚C, total protein was isolated from cells using cold RIPA buffer containing 1% PMSF (Beyotime Institute of Biotechnology). The lysate was collected by centrifugation at 12,000 x g for 10 min at 4˚C. Protein concentrations were determined by performing a bicinchoninic acid assay. Proteins (30 μg) were separated by 10% SDS-PAGE and transferred onto PVDF membranes (Merck KGaA) following electrotransfer at 100 V constant pressure for 90 min. Following blocking with 5% skimmed milk for 1 h at 25˚C, the membranes were incubated at 4˚C for 12 h with primary antibodies targeted against: EGFR (cat. no. 2085), phosphorylated (p)-EGFR (Tyr1068; cat. no. 3777), MMP-2 (cat. no. 40994), MMP-7 (cat. no. 3801), MMP-9 (cat. no. 13667), β-catenin (cat. no. 8480), Vimentin (cat. no. 5741), snail family transcriptional repressor 1 (Snail; cat. no. 3879), E-cadherin (cat. no. 3195), GAPDH (cat. no. 5174), β-actin (cat. no. 4970) and Rac1 (cat. no. 10485-2-AP). All antibodies were rabbit monoclonal antibodies that were used at a dilution of 1:1,000. All antibodies were purchased from Cell Signaling Technology, Inc., except for the Rac1 primary antibody, which was purchased from ProteinTech Group, Inc. Following washing with PBST (0.05% Tween-20) three times (10 min per wash), the membranes were incubated with a HRP-conjugated secondary antibody (cat. no. ab6721; 1:30,000; Abcam) for 1 h at room temperature. Following washing three times with PBST, protein bands were visualized using an Odyssey scanner (LI-COR Biosciences). Protein expression was semi-quantified using ImageJ software (version 1.8.0; National Institutes of Health) with β-actin as the loading control.

For EGF stimulation, cells were incubated with different concentrations of hybrid 7B or gefitinib for 48 h, followed by incubation with EGF (50 ng/ml; cat. no. 236-EG-200) for 20 min at 37˚C.

Molecular docking. To investigate the interaction between compound molecules and EGFR or Rac1 proteins, molecular docking research was conducted using Molecular Operating Environment (MOE; version 10.2008) software provided by Chemical Computing Group ULC. London dG scoring was used to evaluate the binding affinity of each compound to EGFR or Rac1. The lower the score, the more hydrogen bonds, and the tighter the interaction of amino acid residues, which indicated a more stable and stronger interaction between the compound and protein. The protein structures of EGFR [Protein Data Bank (PDB) ID: 3W2S] and Rac1 (PDB ID: 2rmk) were obtained from the protein database Research Collaboratory for Structural Bioinformatics PDB (www.rcsb.org). The chemical structure of Rhein, gefitinib and hybrid 7B were drawn by ChemBio Draw Ultra software (version 12.0; PerkinElmer, Inc.) and saved in PDB format.

Statistical analysis. Comparisons between two groups were analyzed using the unpaired Student's t-test. Comparisons among multiple groups were analyzed using one-way ANOVA followed by Tukey's post hoc test. Data are presented as the mean ± SD of at least three independent experiments. Statistical analyses were performed using SPSS (version 20.0; IBM Corp.) and GraphPad Prism (version 8; GraphPad Software, Inc.) software. $P<0.05$ was considered to indicate a statistically significant difference.

Results

Inhibitory effect of hybrid 7B, Rhein and gefitinib on MDA-MB-231, MCF-7 and MCF-10A cell viability. The MTT assay was performed to assess the effects of hybrid 7B, Rhein and gefitinib on MDA-MB-231 TNBC, MCF-7 breast cancer and MCF-10A normal breast epithelial cell viability. The results indicated that hybrid 7B inhibited MDA-MB-231 and MCF-7 cell viability, displaying significantly lower IC_{50} values compared with Rhein and gefitinib. In normal breast epithelial cells, the IC_{50} value of hybrid 7B was approximately twice that of the IC_{50} value in MDA-MB-231 cells, suggesting that hybrid 7B displayed a certain level of cell selectivity.

In addition, the IC_{30}, IC_{50} and IC_{70} values of MDA-MB-231 were close to 1, 2 and 4 μM, respectively. Moreover, the IC_{30}, IC_{50} and IC_{70} of MCF-7 cells were close to 4, 8 and 16 μM, respectively (Table I). Therefore, 1, 2 and 4 μM were selected for MDA-MB-231 cells and 4, 8 and 16 μM were selected for MCF-7 cells for subsequent experiments.

Hybrid 7B induces MDA-MB-231 and MCF-7 cell apoptosis. To determine the effect of hybrid 7B on breast cancer cell apoptosis, flow cytometry was performed to assess alterations in apoptotic rates following hybrid 7B treatment for 48 h. The apoptotic rates of MDA-MB-231 cells were 5.23±1.44, 46.35±5.34, 77.37±3.55 and 89.37±5.19% following treatment with 0, 1, 2 and 4 μM hybrid 7B, respectively (Fig. 1A). The apoptotic rates of MCF-7 cells were 4.43±0.71, 30.91±4.01, 39.37±3.07 and 51.10±3.84% following treatment with 0, 4, 8 and 16 μM hybrid 7B, respectively (Fig. 1B). Increasing concentrations of hybrid 7B results in increased rates of apoptosis in MDA-MB-231 and MCF-7 cells. The results suggested that hybrid 7B significantly promoted MDA-MB-231 and MCF-7 cell apoptosis compared with the control group. At the same concentration (4 μM), the apoptotic rate of MDA-MB-231 cells was notably higher compared with MCF-7 cells.

MDA-MB-231 cell cycle progression is blocked by hybrid 7B at the G_2/M phase. The cell cycle distribution following hybrid 7B treatment for 48 h was analyzed via flow cytometry. Compared with the control group, the proportion of MDA-MB-231 cells at the S and G_2/M phases was significantly increased by hybrid 7B treatment in a concentration-dependent manner (Fig. 1C), indicating that hybrid 7B blocked MDA-MB-231 cell cycle progression at the S and G_2/M phases. However, no significant differences in the proportion of cells at different cell cycle phases was observed among the control and hybrid 7B groups in MCF-7 cells (Fig. 1D).

MDA-MB-231 and MCF-7 cells display apoptotic morphological alterations following hybrid 7B treatment. TEM is the gold standard for identifying various modes of cell death (12). In the control groups, cells and the nuclear membranes were intact and smooth, the nuclear chromatin displayed a normal distribution, and organelles, including the endoplasmic reticulum, mitochondria and lysosomes, were well developed (Fig. 2A and C). In hybrid 7B-treated MDA-MB-231 (Fig. 2B) and MCF-7 (Fig. 2D) cells, typical morphological alterations of apoptotic cells, including cell shrinkage, irregular nuclei and chromatin concentrated at the edge of the nucleus, swelling of mitochondria, disappearance of cristae, a large number of vacuoles and apoptotic bodies, were observed via TEM.

Table I. Inhibitory concentrations of hybrid 7B, Rhein and gefitinib in breast cancer cells.

A, MDA-MB-231 cells

Compound	IC_{30}	IC_{50}	IC_{70}
Hybrid 7B	1.02±0.23	2.31±0.42[a,b]	4.15±0.35
Rhein	-	163.96±33.36	-
Gefitinib	-	31.73±2.98	-

B, MCF-7 cells

Compound	IC_{30}	IC_{50}	IC_{70}
Hybrid 7B	3.9±0.36	9.02±0.71[a,b]	16.45±1.23
Rhein	-	120.19±10.98	-
Gefitinib	-	29.76±2.04	-

C, MCF-10A cells

Compound	IC_{30}	IC_{50}	IC_{70}
Hybrid 7B	-	5.19±0.81[a,b]	-
Rhein	-	>100	-
Gefitinib	-	0.55±0.12	-

[a]P<0.001 vs. Rhein; [b]P<0.001 vs. gefinitb.

Hybrid 7B modulates mitochondrial membrane potential in MDA-MB-231 and MCF-7 cells. To verify mitochondrial alterations, a JC-1 fluorescent probe was used to further detect the mitochondrial membrane potential of cells. When the mitochondrial membrane potential is high, JC-1 aggregates to form a polymer in the mitochondrial matrix, resulting in red fluorescence. When the mitochondrial membrane potential is low, JC-1 is a monomer and produces green fluorescence. The percentage of MDA-MB-231 cells with red fluorescence was 79.94±2.14, 71.29±2.13, 68.19±3.03 and 40.23±6.00% following treatment with 0, 1, 2 or 4 μM hybrid 7B, respectively (Fig. 3). The percentage of MCF-7 cells with red fluorescence was 87.39±3.88, 71.52±3.22, 69.44±3.87 and 62.02±6.40% following treatment with 0, 4, 8 and 16 μM hybrid 7B, respectively. The results demonstrated that the mitochondrial function of MCF-7 cells was significantly impaired following treatment with hybrid 7B compared with the control group, and the mitochondrial function of MDA-MB-231 cells was significantly impaired at higher concentration of hybrid 7B (2.4 μM).

Hybrid 7B decreases MDA-MB-231 cell migration and invasion by inhibiting EMT. Under the same conditions,

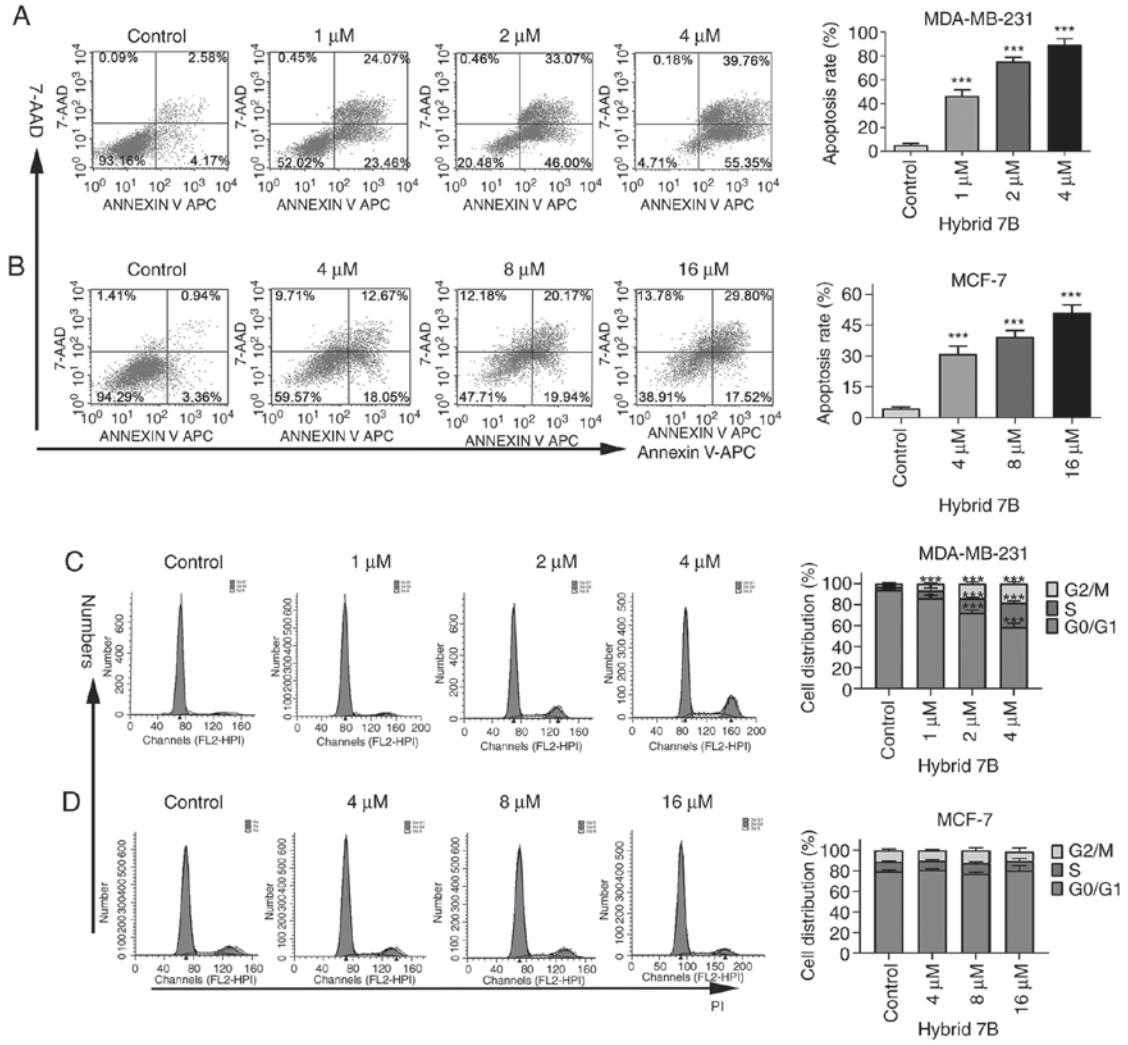

Figure 1. Hybrid 7B affects breast cancer cell apoptosis and cell cycle progression. MDA-MB-231 and MCF-7 cells were treated with different concentrations of hybrid 7B for 48 h. Annexin V-APC/7-AAD staining and flow cytometry were performed to detect (A) MDA-MB-231 and (B) MCF-7 cell apoptosis. Cell cycle distribution was detected by PI staining and flow cytometry in (C) MDA-MB-231 and (D) MCF-7 cells. Data are presented as the mean ± SD of three independent experiments. ***P<0.001 vs. control. APC, allophycocyanin; 7-AAD, 7-aminoactinomycin D.

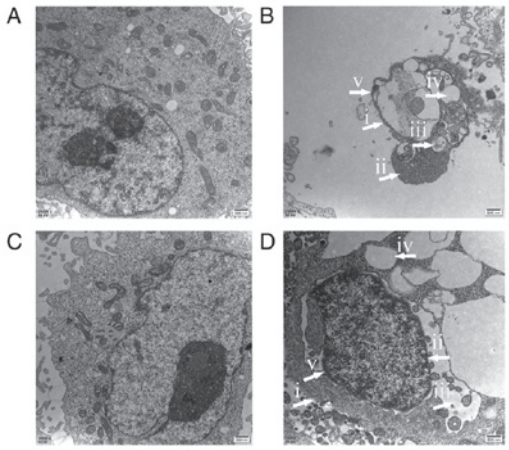

Figure 2. Effect of hybrid 7B on breast cancer cell ultrastructure. (A) MDA-MB-231 cell control group. (B) MDA-MB-231 cell hybrid 7B (2 μM) treatment group. (C) MCF-7 cell control group. (D) MCF-7 cell hybrid 7B (8 μM) group. Compared with the control groups, the hybrid 7B groups displayed typical morphological features of apoptosis: i) Cell shrinkage; ii) irregular nuclei and chromatin concentrated at the edge of the nucleus; iii) swelling of the mitochondria and disappearance of cristae; iv) a large number of vacuoles; and v) apoptotic bodies in the cytoplasm.

the invasive ability of MDA-MB-231 cells was significantly higher compared with MCF-7 cells (Fig. 4A). Therefore, MDA-MB-231 cells were selected for subsequent experiments. To avoid the effect of hybrid 7B on cell viability, non-cytotoxic concentrations of hybrid 7B (0.25, 0.5 and 1 μM), which were determined based on the MTT assay results, were selected for the invasion assay. The number of invading MDA-MB-231 cells was 60.00±12.35, 17.33±10.97 and 8.00±3.56 following treatment with 0.25, 0.5 and 1 μM hybrid 7B, respectively, which was significantly reduced compared with the control group (141.25±19.82; Fig. 4B). Similarly, the wound-healing assay results demonstrated that the wound healing percentage of untreated MDA-MB-231 cells was 95.28±3.04%, whereas following treatment with 0.25, 0.5 and 1 μM hybrid 7B, the wound healing percentages were 85.63±2.28, 70.00±5.21 and 41.27±4.06%, respectively, which were significantly reduced compared with the control group (Fig. 4C). The results indicated that hybrid 7B significantly reduced MDA-MB-231 cell migration and invasion compared with the control group.

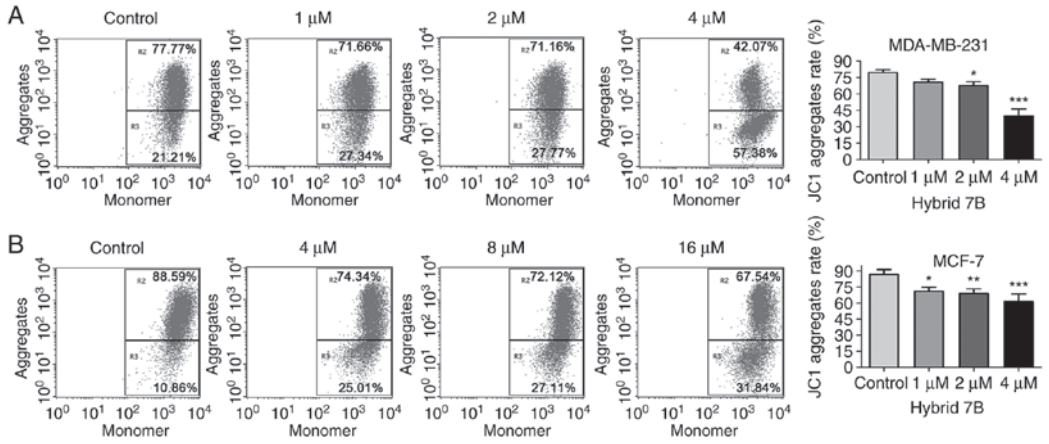

Figure 3. Effect of hybrid 7B on the mitochondrial membrane potential of breast cancer cells. Flow cytometry using JC-1 fluorescent probes was performed to detect alterations in the mitochondrial membrane potential of cells following treatment with hybrid 7B for 48 h. Mitochondrial membrane potential in (A) MDA-MB-231 and (B) MCF-7 cells. Data are presented as the mean ± SD of three independent experiments. *P<0.05, **P<0.01 and ***P<0.001 vs. control.

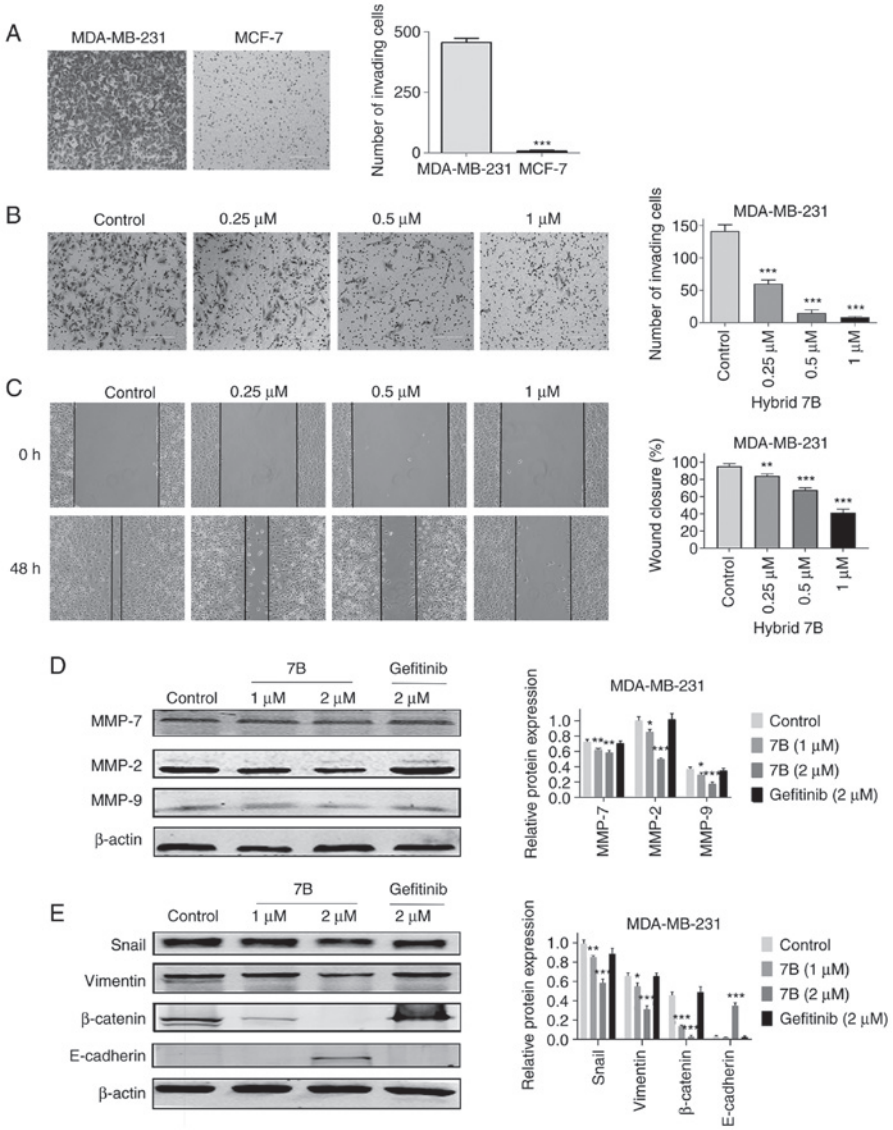

Figure 4. Effect of hybrid 7B on MDA-MB-231 cell invasion, migration and EMT. (A) Comparison between MDA-MB-231 cell invasion and MCF-7 cell invasion (scale bar, 200 μm). (B) Effect of hybrid 7B on MDA-MB-231 cell invasion (scale bar, 200 μm). MDA-MB-231 cells were treated with hybrid 7B (0, 0.25, 0.5 or 1 μM) for 48 h (scale bar, 200 μm). (C) Effect of hybrid 7B on MDA-MB-231 cell migration (magnification, x100). MDA-MB-231 cells were treated with hybrid 7B (0, 0.25, 0.5 or 1 μM) for 48 h. Effect of hybrid 7B on (D) MMP and (E) EMT-related protein expression in MDA-MB-231 cells. Cells were treated with different doses of hybrid 7B or gefitinib for 48 h. *P<0.05, **P<0.01 and ***P<0.001 vs. control. EMT, epithelial-mesenchymal transition; MMP, matrix metallopeptidase; Snail, snail family transcriptional repressor 1; 7B, hybrid 7B.

Table II. Binding affinity and interactions of Rac1-ligand complexes.

Compound	London dG (kcal/mol)	Amino acid involved in H-bonds	Distance of hydrogen bond (Å)	Hydrophobic interactions
Hybrid 7B	-31.215	Thr17	2.90	Ala159, Ala13 and Phe28
		Thr35(3)	2.55/2.60/2.53	Val14, Ala59, Leu67, Pro34, Ile33 and Val36
Rhein	-12.759	Asp118(2)	1.72/2.26	Leu160 and Ala159
		Ala159	2.83	
Gefitinib	-25.953	Gly12	2.96	Phe28, Leu19,V al14, Ala159 and Phe 82
		Lys116	3.06	
		Ala159	2.96	

Table III. Binding affinity and interactions of EGFR-ligand complexes.

Compound	London dG (kcal/mol)	Amino acid involved in H-bonds	Distance of hydrogen bond (Å)	Hydrophobic interactions
Hybrid 7B	-35.325	Met 793	1.56	Leu788, Val26, Leu844, Ala743, Leu718, Leu858, Met766,
		Lys 745(2)	2.66/2.26	Met793, Leu1001, Phe997, Leu792, Pro794 and Met 1002
		Thr 854	2.62	
Rhein	-16.330	Cys 775	1.99	Leu777, Met766, Phe856 Leu747, Leu858, Leu 788
Gefitinib	-27.211	Lys 745	3.40	Leu862, Leu747, Phe856, Leu858, Leu788, Phe723, Ala859, Met766, Leu777 and Val 876

Compared with the control group, hybrid 7B significantly reduced the expression levels of MMP-2, MMP-7 and MMP-9 in MDA-MB-231 cells in a dose-dependent manner (Fig. 4D). In addition, hybrid 7B significantly decreased the expression levels of EMT-related proteins, including β-catenin, vimentin and Snail, and significantly upregulated E-cadherin expression levels compared with the control group. The results indicated that hybrid 7B reversed the EMT process of MDA-MB-231 cells, whereas the positive control gefitinib did not display the same effect.

Docking results of hybrid 7B, Rhein, gefitinib and Rac1. Molecular docking studies of hybrid 7B, Rhein and gefitinib were performed using MOE docking software. The binding modes of hybrid 7B, Rhein, gefitinib and Rac1 are presented in Table II and Fig. 5A. Hybrid 7B formed four hydrogen bonds with amino acid residues Thr17 and Thr35, Rhein formed three hydrogen bonds with amino acid residues Asp118 and Ala159, and gefitinib formed three hydrogen bonds with amino acid residues Gly12, Lys116 and Ala159. The London dG scores of hybrid 7B-Rac1, Rhein-Rac1 and gefitinib-Rac1 complexes were -31.215, -12.759 and -25.953 kcal/mol, respectively (Table II). The higher the negative value, the stronger the binding affinity between the compounds and Rac1; therefore, it was hypothesized that hybrid 7B displayed a stronger ability of targeting and regulating Rac1 compared with Rhein and gefitinib.

Docking results of hybrid 7B, Rhein, gefitinib and EGFR. The London dG scores of 7B-EGFR, Rhein-EGFR and gefitinib-EGFR complexes were -35.325, -16.330 and -27.211 kcal/mol, respectively (Table III and Fig. 5B). The interaction energies of hybrid 7B with EGFR were superior compared with Rhein with EGFR. Hydrogen bonding interactions serve an important role in the stability of a complex. The more hydrogen bonds formed in the complex, the closer the hydrogen bond between the receptor and the ligand, and the more conducive to the stability of the complex (13). The results demonstrated that three hydrogen bonds were observed in hybrid 7B, whereas one hydrogen bond was identified in Rhein. The number of amino acid residues involved in hybrid 7B-EGFR interactions was higher compared with those involved in Rhein-EGFR and gefitinib-EGFR interactions. The results indicated that hybrid 7B bound more tightly and strongly with EGFR compared with Rhein and gefitinib.

Hybrid 7B downregulates the expression levels of Rac1, EGFR and p-EGFR. To further verify whether hybrid 7B displayed targeted regulation of EGFR and Rac1 proteins in breast cancer cells, western blotting was performed to detect their expression level in breast cancer cells treated with hybrid 7B or gefitinib (positive control). The results demonstrated that EGFR and Rac1 expression levels in MDA-MB-231 cells were significantly higher compared with MCF-7 cells (Fig. 6A). EGFR protein was expressed at low levels in MCF-7 cells; therefore, the effect of hybrid 7B on EGFR protein in MCF-7 cells was not investigated.

Compared with the control group, hybrid 7B not only significantly downregulated the expression levels of EGFR

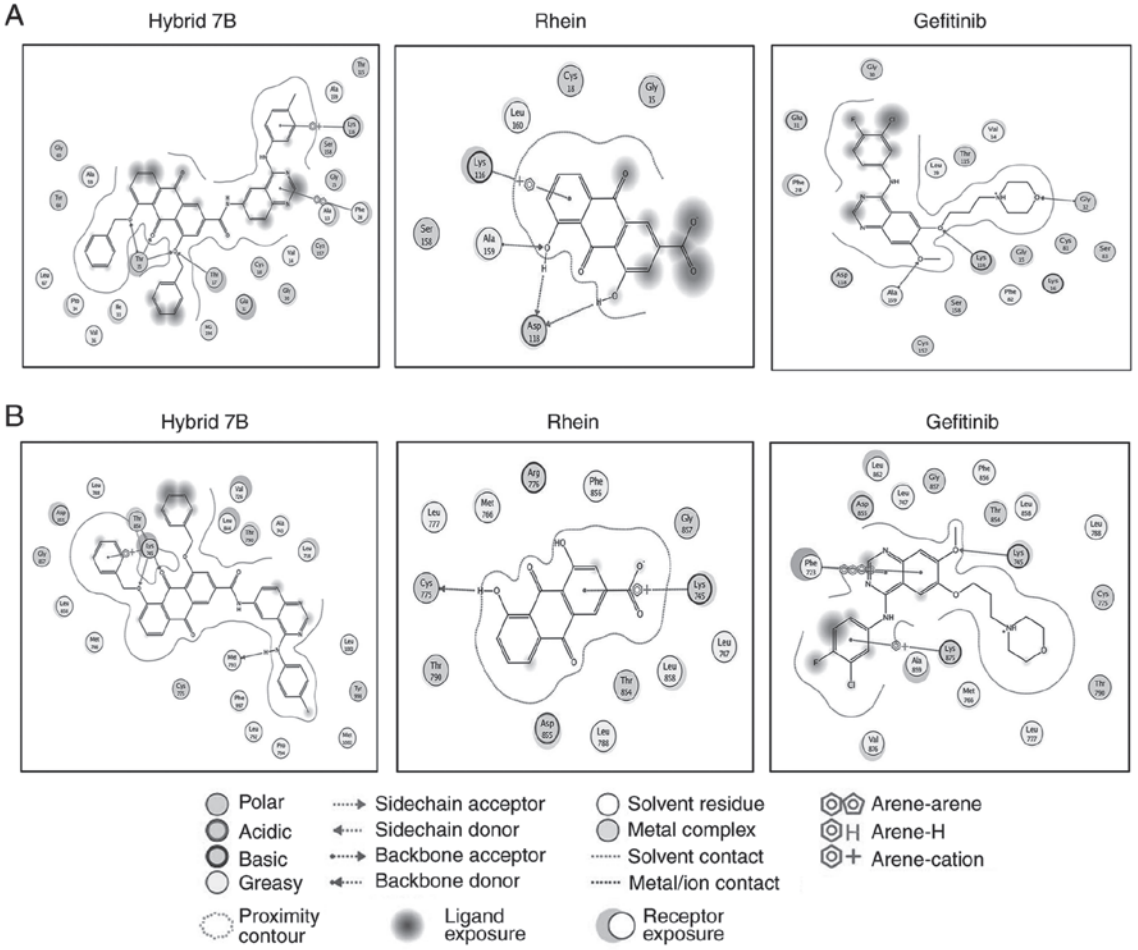

Figure 5. Molecular interactions between compounds and the active sites of Rac1 or EGFR. (A) Rac1-compound complex. (B) EGFR-compound complex.

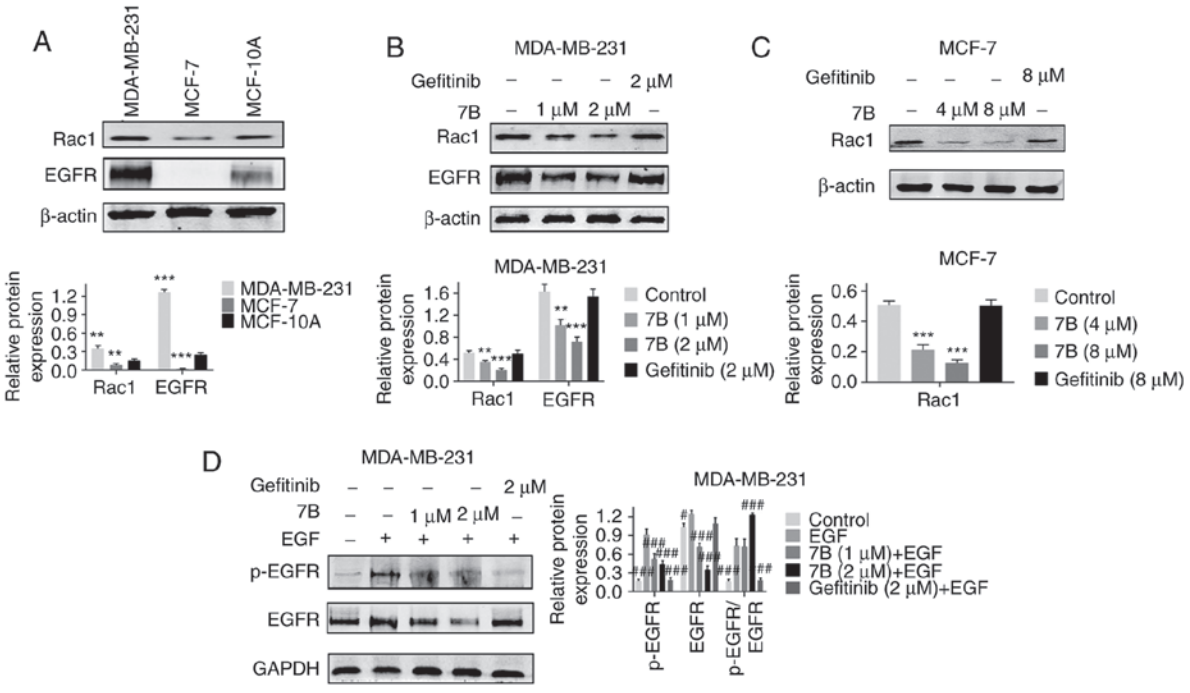

Figure 6. Hybrid 7B and gefitinib alter the protein expression levels of Rac1, EGFR and p-EGFR. EGFR and Rac1 protein expression levels in (A) MDA-MB-231, MCF-7 and MCF-10A cells, (B) MDA-MB-231 cells treated with hybrid 7B or gefitinib, and (C) MCF-7 cells treated with hybrid 7B or gefitinib. (D) EGFR and p-EGFR protein expression levels in MDA-MB-231 cells treated with different concentrations of hybrid 7B or gefitinib, followed by incubation with EGF (50 ng/ml) for 20 min. Data are presented as the mean ± SD of three independent experiments. **P<0.01 and ***P<0.001 vs. control $^{\#}$P<0.05, $^{\#\#}$P<0.01 and $^{\#\#\#}$P<0.001 vs. EGF. p, phosphorylated; 7B, hybrid 7B.

and Rac1 in MDA-MB-231 cells in a dose-dependent manner, but also partially reversed the regulatory effect of EGF on p-EGFR in MDA-MB-231 cells, confirming the targeting effect of hybrid 7B on EGFR (particularly p-EGFR) and Rac1 (Fig. 6B-D).

Discussion

The invasion and metastasis of malignant tumors is a complex, multi-step process that involves the regulation of multiple genes (14). Previous studies have indicated that EGFR is closely associated with tumor cell adhesion, migration, EMT and extracellular matrix (ECM) degradation, and serves an important role in the process of invasion and metastasis (4,15). It has been reported that >50% of patients with TNBC display EGFR overexpression (15), and these patients can undergo EGFR-tyrosine kinase inhibitor (TKI) therapy (16). However, no clear clinical benefit regarding the use of EGFR-targeted TKIs, including gefitinib, erlotinib and cetuximab, has been reported (17,18). One reason for treatment failure may be that the progression of TNBC does not rely solely on the EGFR signaling pathway, but is regulated by several proteins. When EGFR is inhibited, there is an alternative response mechanism dominated by other proteins in patients with breast cancer (19). For instance, it has been reported that Rac1 protein, which is also highly expressed in TNBC, is a component of the signaling pathway and may serve as a therapeutic target for tumor angiogenesis and metastasis (20). Another potential reason for treatment failure may be that the binding mode of EGFR-TKIs and EGFR also affects the curative effect of EGFR-TKIs. Gefitinib, the first generation of oral EGFR-TKIs, has been reported to compete with Mg-ATP binding sites in the EGFR-TK catalytic region, preventing EGFR-induced signal activation. If there is a mutation in the binding site or other compounds competitively bind to the binding site, the antitumor effect of EGFR-TKI is reduced (21). Therefore, the synthesis of novel multi-target EGFR-TKIs, which can inhibit the malignant proliferation and metastasis of TNBC by acting on multiple targets, may serve as a more effective strategy. Inspired by the results of a lung cancer study (22), Rac1-mediated signaling pathways are considered to be independent of other downstream signaling pathways mediated by EGFR, including PI3K/Akt or MEK1/2/ERK1/2 signaling pathways. Rac1 specific inhibitor NSC23766 can inhibit gefitinib-resistant non-small cell lung cancer cell viability and migration, even in the presence of MEK and PI3K inhibitors (22). In addition, it has been reported that Rac1 inhibitor NSC23766 and HER1/EGFR-targeting drug erlotinib display a synergistic antiproliferative effect in glioblastoma (23). Our previous study demonstrated that compounds containing an anthraquinone structure regulated Rac1 expression (9). Simultaneously targeting several signaling pathways is critical; therefore, developing novel combinations targeting both EGFR and Rac1 proteins may serve as an advantageous therapeutic approach. Based on the pharmacophore combination principle, quinazoline and anthraquinone scaffolds were organically fused, and hybrid 7B was synthesized (11).

The results of molecular docking demonstrated that the binding affinities of hybrid 7B to EGFR were stronger compared with gefitinib, suggesting that the binding mode of hybrid 7B to EGFR may not be consistent with that of gefitinib. The western blotting results also indicated that hybrid 7B not only significantly decreased the expression of p-EGFR (Fig. 6D), but also downregulated the expression of EGFR compared with gefitinib (Fig. 6B), which was consistent with the results obtained for the second-generation EGFR-TKI alphatinib (24).

A decrease in the mitochondria membrane potential is a hallmark of apoptosis initiation (25). The JC-1 fluorescent probe assay was used in the present study to assess alterations in the mitochondrial membrane potential following hybrid 7B treatment. Numerous typical morphological features of apoptosis induced by hybrid 7B treatment were verified by TEM, including cell shrinkage, irregular nuclei, swelling of mitochondria, disappearance of cristae, and vacuoles and apoptotic bodies in the cytoplasm. The results indicated that hybrid 7B caused damage to the mitochondrial membrane and decreased the membrane potential compared with the control group.

Increasing evidence has demonstrated that TNBC metastasis is associated with abnormal activation of EMT (26,27). EMT is the process of acquisition of molecular alterations by which epithelial cancer cells lose their epithelial features (E-cadherin and cytokeratin) and gain mesenchymal features (vimentin, N-cadherin, Snail, Slug and Twist) (28). Triple-negative breast cancer cells are transformed by EMT, escape from the primary tumor site, invade the stromal tissues and establish a distant secondary tumor. Epithelial marker E-cadherin protein expression loss and increased mesenchymal marker expression, including β-catenin and vimentin, are features of the EMT phenotype (29). A previous study reported that EGFR-TKI afatinib regulates EMT by inhibiting EGFR, and can significantly reduce MMP-9 protein expression levels (30). Rac1 expression is also associated with EMT, thus inhibiting Rac1 expression in gastric adenocarcinoma cells blocks EMT, invasion and metastasis (31). Therefore, regulating the expression of EGFR and Rac1 proteins may reverse the EMT process of tumor cells. The results of the present study demonstrated that hybrid 7B successfully reversed the EMT of MDA-MB-231 by significantly downregulating the expression levels of β-catenin and Vimentin, and significantly upregulating the expression levels of E-cadherin compared with the control group. At the same concentration (2 μM), the ability of hybrid 7B to reverse EMT was notably superior compared with gefitinib, which may be associated with synergistic inhibition of the expression of multiple proteins. Therefore, it was hypothesized that hybrid 7B may serve as a potential multi-target antitumor activity compound.

MMPs are a group of calcium-dependent extracellular proteases that facilitate ECM degradation, resulting in tumor invasion and metastasis promotion. MMP expression is regulated by EMT-related signal transduction pathways, including the TGF-β signaling pathway (32). In HT1080 fibrosarcoma cells cultured in three-dimensional collagen gel, Rac1 mediated MMP-2 activation and MMP14 expression/processing during the encounter between invading tumor cells and type I collagen-rich stroma, thereby facilitating collagenolysis and cell invasion (33). Using specific inhibitors, Binker *et al* (34) revealed that not only is Rac1 activated following the lipopolysaccharide stimulation of NCI-H292 cells (human

airway cells), but also that PI3K was the signaling molecule downstream of EGFR that regulated Rac1 activity. In addition, a study has reported that EGFR overexpression in tumor cells is involved in MMP-9 upregulation (35). Therefore, the aforementioned studies indicated that the occurrence of EMT, tumor invasion and metastasis is closely associated with the expression of EGFR, Rac1 and MMPs. The results of the present study demonstrated that following treatment with hybrid 7B, the protein expression levels of MMP-2, MMP-7, MMP-9, EGFR and Rac1 were significantly decreased in MDA-MB-231 cells compared with the control group. In addition, MDA-MB-231 cell invasion and metastasis were significantly inhibited by hybrid 7B treatment compared with the control group. The aforementioned results further verified the multi-target antitumor activity of hybrid 7B.

In the present study, the results demonstrated that MDA-MB-231 cell cycle progression was blocked at the S and G_2/M phases, but there was no alteration in MCF-7 cell cycle progression following hybrid 7B treatment. The aforementioned result was similar to the findings reported by Elkhalifa *et al* (36). In the aforementioned study, compound 14 induced apoptosis in MDA-MB-231 and MCF-7 cells, and MDA-MB-231 cells displayed cell cycle arrest at the G_2/M phase, whereas the MCF-7 cell cycle was not altered. However, in the present study, the sub-G_0/G_1 peak was not identified by flow cytometry in these two cell lines. Since any fractional DNA content, not only that caused by apoptosis but also that caused by other reasons, can result in multiple nuclear fragments, it has been suggested that the sub-G_1 peak is not a good indicator of cell apoptosis and cannot fully represent the number of apoptotic cells. Therefore, the apoptosis peak was not modeled using ModFitLT software to analyze the cell cycle data in the present study, thus a hypodiploid peak (sub-G1 peak) was not presented in the present study.

Moreover, the results of the present study demonstrated that compared with MDA-MB-231 cells, EGFR protein expression in MCF-7 cells was notably lower, indicating that MCF-7 cells could not invade the matrix. This result was consistent with the conclusions of two previous studies (2,37) that reported that $EGFR^+$ cancer cell lines were more invasive compared with $EGFR^-$ cells. The aforementioned result also provided a potential explanation for why the IC_{50} value of hybrid 7B was markedly higher in MCF-7 compared with MDA-MB-231 cells due to the lack of an EGFR target in MCF-7.

In the present study, the inhibitory effect of hybrid 7B on TNBC cell viability and metastasis was only studied *in vitro*. However, the possible signaling pathway underlying hybrid 7B-induced suppression of cell migration, invasion and EMT in MDA-MB-231 cells requires further investigation, including *in vivo* studies.

In conclusion, the present study demonstrated that hybrid 7B induced breast cancer cell apoptosis, arrested MDA-MB-231 cell cycle progression at the G_2/M phase, and significantly inhibited TNBC invasion and metastasis compared with the control group. The mechanism underlying hybrid 7B was associated with downregulation of EGFR and Rac1 protein expression levels and reversal of TNBC EMT. Therefore, the results of the present study indicated that hybrid 7B may serve as a potential dual-target inhibitor of EGFR and Rac1.

Acknowledgements

Not applicable.

Funding

The present study was supported by the Guangxi Natural Science Foundation (grant no. 2018GXNSFAA281064), the Innovation Project of Guangxi Graduate Education (grant no. YCSW2019107) and the Program of Key Laboratory of High-Incidence Tumor Prevention and Treatment (Guangxi Medical University) and the Ministry of Education (China; grant no. GK2019-22).

Availability of data and materials

The datasets used and/or analyzed during the current study are available from the corresponding author on reasonable request.

Authors' contributions

JK, HH and DL conceived and designed the experiments. JK, WT, JL, XL and LZ performed the experiments. JK and YZ analyzed the data. WT, JL and LZ contributed reagents, materials and analysis tools. JK, YZ and DL drafted the manuscript. JK and DL confirm the authenticity of all the raw data. All authors read and approved the manuscript.

Ethics approval and consent to participate

Not applicable.

Patient consent for publication

Not applicable.

Competing interests

The authors declare that they have no competing interests.

References

1. Yin L, Duan JJ, Bian XW and Yu SC: Triple-negative breast cancer molecular subtyping and treatment progress. Breast Cancer Res 22: 61, 2020.
2. McGovern UB, Francis RE, Peck B, Guest SK, Wang J, Myatt SS, Krol J, Kwok JM, Polychronis A, Coombes RC and Lam EW: Gefitinib (Iressa) represses FOXM1 expression via FOXO3a in breast cancer. Mol Cancer Ther 8: 582-591, 2009.
3. Lehmann BD, Bauer JA, Chen X, Sanders ME, Chakravarthy AB, Shyr Y and Pietenpol JA: Identification of human triple-negative breast cancer subtypes and preclinical models for selection of targeted therapies. J Clin Invest 121: 2750-2767, 2011.
4. Matsuda N, Lim B, Wang X and Ueno NT: Early clinical development of epidermal growth factor receptor targeted therapy in breast cancer. Expert Opin Investig Drugs 26: 463-479, 2017.
5. Peng B, He R, Xu Q, Yang Y, Hu Q, Hou H, Liu X and Li J: Ginsenoside 20(S)-protopanaxadiol inhibits triple-negative breast cancer metastasis in vivo by targeting EGFR-mediated MAPK pathway. Pharmacol Res 142: 1-13, 2019.
6. Gonzalez-Conchas GA, Rodriguez-Romo L, Hernandez-Barajas D, Gonzalez-Guerrero JF, Rodriguez-Fernandez IA, Verdines-Perez A, Templeton AJ, Ocana A, Seruga B, Tannock IF, *et al*: Epidermal growth factor receptor overexpression and outcomes in early breast cancer: A systematic review and a meta-analysis. Cancer Treat Rev 62: 1-8, 2018.

7. Payapilly A and Malliri A: Compartmentalisation of RAC1 signalling. Curr Opin Cell Biol 54: 50-56, 2018.
8. Su Z, Li Z, Wang C, Tian W, Lan F, Liang D, Li J, Li D and Hou H: A novel Rhein derivative: Activation of Rac1/NADPH pathway enhances sensitivity of nasopharyngeal carcinoma cells to radiotherapy. Cell Signal 54: 35-45, 2019.
9. Zhou G, Peng F, Zhong Y, Chen Y, Tang M and Li D: Rhein suppresses matrix metalloproteinase production by regulating the Rac1/ROS/MAPK/AP-1 pathway in human ovarian carcinoma cells. Int J Oncol 50: 933-941, 2017.
10. Roskoski R Jr: ErbB/HER protein-tyrosine kinases: Structures and small molecule inhibitors. Pharmacol Res 87: 42-59, 2014.
11. Liang D, Su Z, Tian W, Li J, Li Z, Wang C, Li D and Hou H: Synthesis and screening of novel anthraquinone-quinazoline multitarget hybrids as promising anticancer candidates. Future Med Chem 12: 111-126, 2020.
12. Klöditz K and Fadeel B: Three cell deaths and a funeral: Macrophage clearance of cells undergoing distinct modes of cell death. Cell Death Discov 5: 65, 2019.
13. Daddam JR, Dowlathabad MR, Panthangi S and Jasti P: Molecular docking and P-glycoprotein inhibitory activity of flavonoids. Interdiscip Sci 6: 167-175, 2014.
14. Stivarou T and Patsavoudi E: Extracellular molecules involved in cancer cell invasion. Cancers (Basel) 7: 238-265, 2015.
15. Williams CB, Soloff AC, Ethier SP and Yeh ES: Perspectives on epidermal growth factor receptor regulation in triple-negative breast cancer: Ligand-mediated mechanisms of receptor regulation and potential for clinical targeting. Adv Cancer Res 127: 253-281, 2015.
16. Sporikova Z, Koudelakova V, Trojanec R and Hajduch M: Genetic markers in triple-negative breast cancer. Clin Breast Cancer 18: e841-e850, 2018.
17. Al-Mahmood S, Sapiezynski J, Garbuzenko OB and Minko T: Metastatic and triple-negative breast cancer: Challenges and treatment options. Drug Deliv Transl Res 8: 1483-1507, 2018.
18. Baselga J, Albanell J, Ruiz A, Lluch A, Gascón P, Guillém V, González S, Sauleda S, Marimón I, Tabernero JM, *et al*: Phase II and tumor pharmacodynamic study of gefitinib in patients with advanced breast cancer. J Clin Oncol 23: 5323-5333, 2005.
19. El Guerrab A, Bamdad M, Bignon YJ, Penault-Llorca F and Aubel C: Co-targeting EGFR and mTOR with gefitinib and everolimus in triple-negative breast cancer cells. Sci Rep 10: 6367, 2020.
20. Bid HK, Roberts RD, Manchanda PK and Houghton PJ: RAC1: An emerging therapeutic option for targeting cancer angiogenesis and metastasis. Mol Cancer Ther 12: 1925-1934, 2013.
21. Shi Y, Su C, Cui W, Li H, Liu L, Feng B, Liu M, Su R and Zhao L: Gefitinib loaded folate decorated bovine serum albumin conjugated carboxymethyl-beta-cyclodextrin nanoparticles enhance drug delivery and attenuate autophagy in folate receptor-positive cancer cells. J Nanobiotechnology 12: 43, 2014.
22. Kaneto N, Yokoyama S, Hayakawa Y, Kato S, Sakurai H and Saiki I: RAC1 inhibition as a therapeutic target for gefitinib-resistant non-small-cell lung cancer. Cancer Sci 105: 788-794, 2014.
23. Kim H, Samuel SL, Zhai G, Rana S, Taylor M, Umphrey HR, Oelschlager DK, Buchsbaum DJ and Zinn KR: Combination therapy with anti-DR5 antibody and tamoxifen for triple negative breast cancer. Cancer Biol Ther 15: 1053-1060, 2014.
24. Chen Y, Chen X, Ding X and Wang Y: Afatinib, an EGFR inhibitor, decreases EMT and tumorigenesis of Huh-7 cells by regulating the ERK-VEGF/MMP9 signaling pathway. Mol Med Rep 20: 3317-3325, 2019.
25. Kim TI, Kim H, Lee DJ, Choi SI, Kang SW and Kim EK: Altered mitochondrial function in type 2 granular corneal dystrophy. Am J Pathol 179: 684-692, 2011.
26. Neelakantan D, Zhou H, Oliphant MUJ, Zhang X, Simon LM, Henke DM, Shaw CA, Wu MF, Hilsenbeck SG, White LD, *et al*: EMT cells increase breast cancer metastasis via paracrine GLI activation in neighbouring tumour cells. Nat Commun 8: 15773, 2017.
27. Nieto MA, Huang RY, Jackson RA and Thiery JP: EMT: 2016. Cell 166: 21-45, 2016.
28. Kim S and Lee JW: Membrane proteins involved in epithelial-mesenchymal transition and tumor invasion: Studies on TMPRSS4 and TM4SF5. Genomics Inform 12: 12-20, 2014.
29. Jang MH, Kim HJ, Kim EJ, Chung YR and Park SY: Expression of epithelial-mesenchymal transition-related markers in triple-negative breast cancer: ZEB1 as a potential biomarker for poor clinical outcome. Hum Pathol 46: 1267-1274, 2015.
30. Tien Y, Tsai CL, Hou WH, Chiang Y, Hsu FM, Tsai YC and Cheng JC: Targeting human epidermal growth factor receptor 2 enhances radiosensitivity and reduces the metastatic potential of Lewis lung carcinoma cells. Radiat Oncol 15: 58, 2020.
31. Yoon C, Cho SJ, Chang KK, Park DJ, Ryeom SW and Yoon SS: Role of Rac1 pathway in epithelial-to-mesenchymal transition and cancer stem-like cell phenotypes in gastric adenocarcinoma. Mol Cancer Res 15: 1106-1116, 2017.
32. Santibanez JF, Obradović H, Kukolj T and Krstić J: Transforming growth factor-β, matrix metalloproteinases, and urokinase-type plasminogen activator interaction in the cancer epithelial to mesenchymal transition. Dev Dyn 247: 382-395, 2018.
33. Zhuge Y and Xu J: Rac1 mediates type I collagen-dependent MMP-2 activation. Role in cell invasion across collagen barrier. J Biol Chem 276: 16248-16256, 2001.
34. Binker MG, Binker-Cosen AA, Richards D, Oliver B and Cosen-Binker LI: LPS-stimulated MUC5AC production involves Rac1-dependent MMP-9 secretion and activation in NCI-H292 cells. Biochem Biophys Res Commun 386: 124-129, 2009.
35. Cox G, Jones JL and O'Byrne KJ: Matrix metalloproteinase 9 and the epidermal growth factor signal pathway in operable non-small cell lung cancer. Clin Cancer Res 6: 2349-2355, 2000.
36. Elkhalifa D, Siddique AB, Qusa M, Cyprian FS, El Sayed K, Alali F, Al Moustafa AE and Khalil A: Design, synthesis, and validation of novel nitrogen-based chalcone analogs against triple negative breast cancer. Eur J Med Chem 187: 111954, 2020.
37. Martin JL, de Silva HC, Lin MZ, Scott CD and Baxter RC: Inhibition of insulin-like growth factor-binding protein-3 signaling through sphingosine kinase-1 sensitizes triple-negative breast cancer cells to EGF receptor blockade. Mol Cancer Ther 13: 316-328, 2014.